THE JOURNAL OF BIOLOGICAL CHEMISTRY
Vol. 277, No. 43, Issue of October 25, pp. 41140–41146, 2002
Printed in U.S.A.
© 2002 by The American Society for Biochemistry and Molecular Biology, Inc.

PDZ7 of Glutamate Receptor Interacting Protein Binds to Its Target via a Novel Hydrophobic Surface Area*

Received for publication, July 18, 2002, and in revised form, August 19, 2002
Published, JBC Papers in Press, August 23, 2002, DOI 10.1074/jbc.M207206200

Wei Feng, Jing-Song Fan, Ming Jiang, Ya-Wei Shi, and Mingjie Zhang‡

From the Department of Biochemistry, Hong Kong University of Science and Technology, Clear Water Bay, Kowloon, Hong Kong, People's Republic of China

Glutamate receptor interacting protein 1 (GRIP1) is a scaffold protein composed of seven PDZ (Postsynaptic synaptic density-95/Discs large/Zona occludens-1) domains. The protein plays important roles in the synaptic targeting of α-amino-3-hydroxy-5-methyl-4-isoxazole-propionic acid (AMPA) receptors. The interaction between GRIP1 PDZ7 and a Ras guanine nucleotide exchange factor, GRASP-1, regulates synaptic distribution of AMPA receptors. Here, we describe the three-dimensional structure of GRIP1 PDZ7 determined by NMR spectroscopy. GRIP1 PDZ7 contains a closed carboxyl group-binding pocket and a narrow αB/βB-groove that is not likely to bind to classical PDZ ligands. Unexpectedly, GRIP1 PDZ7 contains a large solvent-exposed hydrophobic surface at a site distinct from the conventional ligand-binding αB/βB-groove. NMR titration experiments show that GRIP1 PDZ7 binds to GRASP-1 via this hydrophobic surface. Our data uncover a novel PDZ domain-mediated protein interaction mode that may be responsible for multimerization of other PDZ domain-containing scaffold proteins.

Postsynaptic synaptic density-95/Discs large/Zona occludens-1 (PDZ)[1] domains are among the most abundant protein-interacting modules in the genomes of metazoans (1). PDZ domain containing proteins have been shown to play important roles in diverse cellular processes including receptor/ion channel clustering, signaling complex assembly, and protein targeting (2–4). A typical PDZ domain contains ~90 amino acid residues folded into a compact globular structure comprising a six-stranded β-barrel flanked by two α-helices (5, 6). The majority of PDZ domain-mediated interactions involves the binding of short peptide fragments located at the extreme carboxyl termini of target proteins to grooves formed by the second α-helix (αB) and the second β-strand (βB) of the PDZ domains (6–9). The carboxyl peptide augments the βB strand in an anti-parallel fashion. Amino acid residues at the 0 and −2 positions of the carboxyl peptide play dominant roles in the peptide binding to a cognate PDZ domain, although residues at the −1 and −3 positions and those at further upstream positions also contribute to the binding (10). In addition to binding to carboxyl peptides, PDZ domains can also use the αB/βB-target-binding groove to interact with internal short peptide fragments with defined structures (9, 11, 12).

Glutamate receptor-interacting protein 1 (GRIP1) contains seven PDZ domains and interacts through PDZ4 and PDZ5 with the COOH-terminal "ESVKI" sequence of the GluR2/3 subunits of AMPA receptors (13, 14). GRIP1 has several closely related gene products, GRIP2 and AMPA receptor binding protein (ABP), and they are all able to bind to AMPA receptors (15, 16). In addition, the GRIP family proteins can interact through PDZ6 with EphB2/EphA7 receptor tyrosine kinase and the ephrinB1 ligand (17–19). Genetic studies have shown that *GRIP1*$^{-/-}$ mice are embryonic lethal, and the mutant embryos develop abnormalities in the dermo-epidermal junction (20). GRIP1 additionally interacts through its PDZ7 with GRASP-1, a Ras guanine-nucleotide exchange factor that regulates the synaptic distribution of AMPA receptors (21). The interaction between GRIP1 PDZ7 and GRASP-1 is rather unusual, as GRASP-1 does not contain obvious PDZ-interacting sequence at its carboxyl terminus. Biochemical analysis has indicated that a 100-residue fragment located at the COOH-terminal end of GRASP-1 is responsible for the interaction of the protein with GRIP1 (21).

The solution structure of the PDZ7 of GRIP1 determined in this study shows that the conventional target-binding groove formed by the αB helix and the βB strand adopts a closed conformation that is not likely to be capable of interacting with carboxyl peptides. Unexpectedly, GRIP1 PDZ7 contains a solvent-exposed hydrophobic surface formed by the βE strand, the αB helix, and the loop connecting the two secondary structural elements. We show that GRIP1 PDZ7 interacts with GRASP-1 via this hydrophobic surface. The data presented in this study uncover a novel mode of PDZ domain-mediated protein-protein interaction.

MATERIALS AND METHODS

Expression and Purification of GRIP1 PDZ7 and GRIP-binding Domain of GRASP-1—The seventh PDZ domain of rat GRIP1 (amino acid residues 980–1070) and the COOH-terminal 100-residue fragment of rat GRASP-1 were polymerase chain reaction-amplified from the respective full-length cDNAs of the proteins with specific primers. The amplified DNA fragments were inserted into a modified version of pET32a (Novagen) in which the DNA sequences encoding the S-tag and thioredoxin were removed. The resulting recombinant plasmid harboring the respective target genes were individually transformed into *Escherichia coli* BL21(DE3) host cells for large scale protein productions. Uniformly ^{15}N- and $^{15}N/^{13}C$-labeled proteins were prepared by

* This work is partially supported by Grants HKUST6198/99M, 6207/00M, and 6097/01M from the Research Grants Council of Hong Kong (to M. Z.) and Grant RG0068/2000-M from the Human Frontiers Science Program. The NMR spectrometers used in this work were purchased using funds donated to the Biotechnology Research Institute of Hong Kong University of Science and Technology (HKUST) by the Hong Kong Jockey Club. The costs of publication of this article were defrayed in part by the payment of page charges. This article must therefore be hereby marked "*advertisement*" in accordance with 18 U.S.C. Section 1734 solely to indicate this fact.

The atomic coordinates and structure factors (code 1M5Z) have been deposited in the Protein Data Bank, Research Collaboratory for Structural Bioinformatics, Rutgers University, New Brunswick, NJ (http://www.rcsb.org/).

‡ Member of the Molecular Neuroscience Center, HKUST. To whom correspondence should be addressed. Tel.: 852-2358-8709; Fax: 852-2358-1552; E-mail: mzhang@ust.hk.

[1] The abbreviations used are: PDZ, Postsynaptic density-95/Discs large/Zona occludens-1; PSD-95, postsynaptic density-95; GRIP, glutamate receptor-interacting protein 1; NOE, nuclear Overhauser effect.

This paper is available on line at http://www.jbc.org

Downloaded from www.jbc.org at Hong Kong University of Science & Technology, on April 9, 2011

growing bacteria in M9 minimal medium using $^{15}NH_4Cl$ (1 g/liter) and $^{13}C_6$-glucose (1 g/liter) as stable isotope sources.

Recombinant GRIP1 PDZ7 and GRASP-1 fragment were purified by a combination of nickel-nitrilotriacetic acid affinity column (Qiagen) followed by gel filtration chromatography. The purified recombinant proteins contained an NH_2-terminal His tag carried over from the cloning vector.

NMR Experiments—Four NMR samples were prepared for structural determination of GRIP1 PDZ7 with a protein concentration of ~1.0 mM (unlabeled PDZ7 in 99.9% D_2O, ^{15}N-labeled protein in 90% H_2O/10% D_2O, two $^{15}N/^{13}C$-labeled samples in 99.9% D_2O and in 90% H_2O/10% D_2O). The protein was dissolved in 100 mM potassium phosphate buffer at pH 6.5 (direct meter reading). The ^{15}N-labeled sample in 90% H_2O/10% D_2O was also used for backbone relaxation data measurements.

All of the NMR experiments were carried out at 25 °C on Varian Inova 500 and 750 spectrometers equipped with 5 mm *z*-shielded gradient triple resonance probes. NMR spectra were processed with the nmrPipe software package (22) and analyzed using PIPP (23) and Sparky (www.cgl.ucsf.edu/home/sparky/). Sequential backbone resonance assignments of the protein were obtained by standard heteronuclear correlation experiments including HNCO, HNCACB, and CBCA(CO)NH and confirmed by a three-dimensional ^{15}N-separated NOESY experiment (24, 25). The non-aromatic non-exchangeable side-chain assignments were obtained using an HCCH-TOCSY experiment. The side chains of the aromatics were assigned by ^1H two-dimensional TOCSY and NOESY experiments with an unlabeled protein sample in D_2O (26). The $-NH_2$ side chains of Asn and Gln residues were assigned by a three-dimensional ^{15}N-separated NOESY experiment with the ^{15}N-labeled protein dissolved in H_2O.

The pulse sequences used to obtain the ^{15}N-longitudinal relaxation times, T_1, the ^{15}N spin-lattice relaxation times, T_2, and the ^1H-^{15}N steady-state NOE values were described previously (27). All of the data were processed using nmrPipe and nmrDraw software (22), and the peak intensities were characterized as peak heights using the Sparky software. The relaxation data were fitted using the Modelfree 4.0 program (provided by A.G. Palmer).

Structural Calculations—Approximate interproton distance restraints were derived from three NOESY spectra (a ^1H two-dimensional homonuclear NOESY, a ^{15}N-separated NOESY, and a ^{13}C-separated NOESY). NOEs were grouped into three distance ranges of 1.8–2.7 Å (1.8–2.9 Å for NOEs involving NH protons), 1.8–3.3 Å (1.8–3.5 Å for NOEs involving NH protons), and 1.8–5.0 Å, respectively, corresponding to strong, medium, and weak NOEs. Hydrogen-bonding restraints (two per hydrogen bond where r_{NH-O} = 1.8–2.2 Å and r_{N-O} = 2.2–3.3 Å) were generated from the standard secondary structure of the protein based on the NOE patterns and backbone secondary chemical shifts. Backbone dihedral angle restraints (ϕ and ψ angles) were derived from $^3J_{HN\alpha}$ coupling constants measured using an HNHA experiment and the backbone chemical shift analysis program TALOS (28). Structures were calculated using the program CNS (29).

Coordinates—The coordinates of the structures of GRIP1 PDZ7 have been deposited in the Protein Data Bank (PDB code 1M5Z), and the chemical shift assignments of PDZ7 have been deposited in the BioMagResBank (accession number 5499).

TABLE I
Structural statistics for the family of 20 structures[a]

Distance restraints	
Intraresidue (i–j = 0)	596
Sequential ($\|i$–$j\|$ = 1)	376
Medium range (2 < $\|i$–$j\|$ < 4)	225
Long range ($\|i$–$j\|$ > 5)	447
Hydrogen bonds	56
Total	1700
Dihedral angle restraints	
Φ	52
Ψ	52
$^3J_{HN\alpha}$ coupling constants	22
Total	126
Mean r.m.s. deviations from the experimental restraints	
Distance (Å)	0.013 ± 0.001
Dihedral angle (Å)	0.228 ± 0.032
3-bond J coupling (Å)	0.468 ± 0.041
Mean r.m.s. deviations from idealized covalent geometry	
Bond (Å)	0.002 ± 0.000
Angle (Å)	0.355 ± 0.010
Improper (Å)	0.186 ± 0.011
Mean energies (kcal mol^{-1})	
E_{NOE}[b]	23.38 ± 3.55
E_{cdih}[b]	0.33 ± 0.09
E_{L-J}	−260.60 ± 14.76
Ramachandran plot[c]	
Residues 980–1070	
% residues in the most favorable regions	75.9
additional allowed regions	19.5
generously allowed regions	3.9
Atomic r.m.s. differences (Å)[d] (Residues 985–992, 1002–1007, 1012–1018, 1023–1027, 1034–1038, 1041–1042, 1048–1056, 1061–1068 in protein)	
Backbone heavy atoms (N, C^α, and C′)	0.31
Heavy atoms	0.81

[a] None of the structures exhibits distance violations greater than 0.3 Å or dihedral angle violations greater than 4°.
[b] The final values of the square-well NOE and dihedral angle potentials were calculated with force constants of 50 kcal mol^{-1} Å^{-2} and 200 kcal mol^{-1} rad^{-2}, respectively.
[c] The program Procheck (38) was used to assess the overall quality of the structures.
[d] The precision of the atomic coordinates is defined as the average r.m.s. difference between the 20 final structures and the mean coordinates of the protein.

RESULTS AND DISCUSSION

Structural Determination—To investigate the mechanism of the interaction between GRIP1 and GRASP-1, we determined the three-dimensional structure of GRIP1 PDZ7 by NMR spectroscopy. A total of 1826 experimentally derived distance and torsion angle restraints allowed us to determine the three-dimensional structure of PDZ7 with high precision (Table I). Fig. 1*A* shows a stereoview of the best-fit superposition of a family of 20 structures of PDZ7. As expected, PDZ7 adopts a typical PDZ domain conformation consisting of six β-strands (from βA to βF) and two α-helices (αA and αB) (Fig. 1*B*). A comparison of the structures of PDZ7 and PDZ2 of PSD-95 using the respective secondary structural elements shows a root mean square difference of 1.57 Å.

The αB/βB-Groove of GRIP1 PDZ7 Adopts a Closed Conformation—The amino acid sequence analysis reveals that PDZ7 from the GRIP family proteins (GRIP1/2 and ABP) have very high sequence identities with one another. The amino acid sequence of PDZ7 is also highly conserved throughout the evolution (Fig. 2). In contrast, the rest of PDZ domains in the data base have rather limited amino acid sequence identities with that of PDZ7 (the PDZ1 of *Calliphora vicina* InaD has the highest sequence identity with GRIP1 PDZ7 of 37%). We further note that the amino acid residue in the first residue of the αB helix (αB1) of GRIP PDZ7 is an absolutely conserved Cys residue (Cys-1048). A data base search revealed that no other known PDZ domains contain a Cys residue in the αB1 position (1). The amino acid residue in the αB1 position is known to play a critical role in recognizing the −2 residue in target carboxyl peptides (6, 10). We analyzed the structural features of this residue as well as the αB/βB-groove in detail, hoping to gain insight into the potential target-binding mechanism of this PDZ domain. Fig. 3*A* compares the conformation of the αB/βB-grooves of PDZ7 and PSD-95 PDZ2. The side chain of Cys-1048 in GRIP1 PDZ7 is packed with hydrophobic residues from both αB and βB (see an example of NOE contacts between Cys-1048 β-protons and side chains of Val-1004, Val-1013, and Val-1052 in Fig. 4*A*). Because of the relatively small size of Cys-1048, the NH_2-terminal end of αB in PDZ7 is slightly closer to βB with respect to the αB helix in PSD-95 PDZ2. In addition, the whole αB-helix rotates ~18° anti-clockwise toward βB (Fig. 3*A*), resulting in a significantly smaller αB/βB-groove. The size of the αB/βB-groove in PDZ7 is not likely to accommo-

Downloaded from www.jbc.org at Hong Kong University of Science & Technology, on April 9, 2011

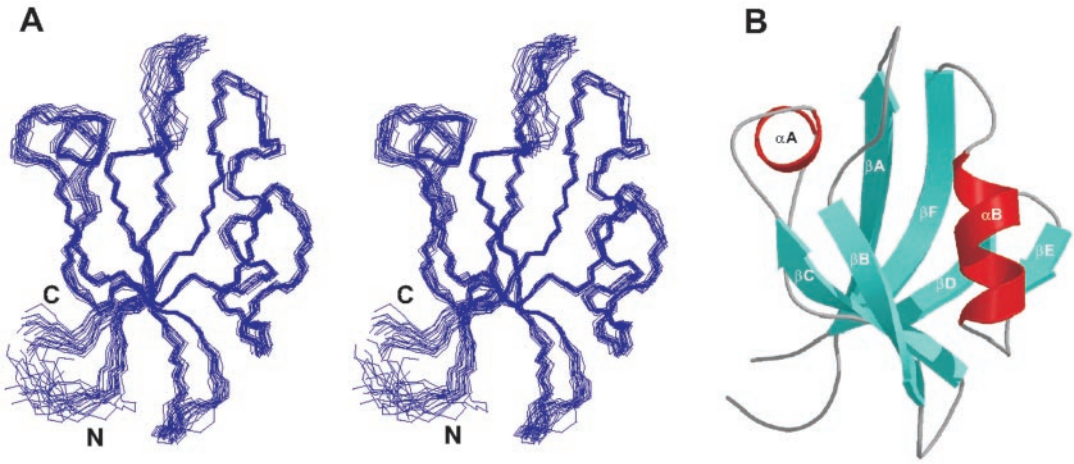

FIG. 1. **Three-dimensional structure of GRIP1 PDZ7 determined by NMR spectroscopy.** *A*, stereoview showing the best-fit superposition of the backbone atoms (N, Cα, and C′) of the final 20 structures of PDZ7. The structures are superimposed against the average structure using the residues 985–1007 and 1012–1068. The NH_2 and COOH termini of the PDZ domain are labeled. The program MOLMOL (34) was used to generate the figure. *B*, *ribbon diagram* of the GRIP1 PDZ7 structure. The secondary structural elements are labeled following the scheme used in the crystal structure of PSD-95 PDZ3 (6). The figure is generated using MOLSCRIPT (35) and Raster3D (36).

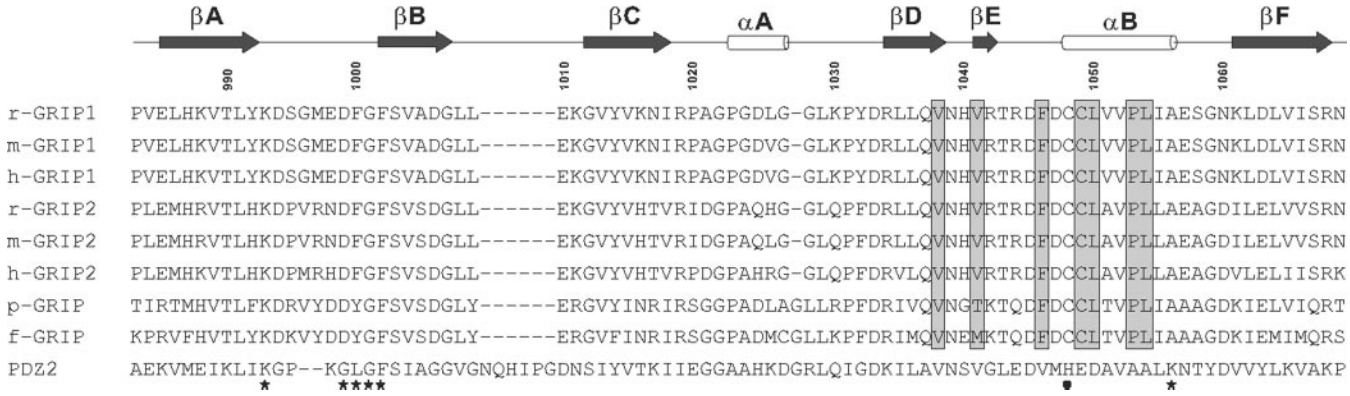

FIG. 2. **Amino acid sequence alignment of the PDZ7 domains of the GRIP family proteins.** The secondary structure of GRIP1 PDZ7 determined from this work is indicated at the *top* of the sequences. For comparison, the amino acid sequence of PSD-95 PDZ2 is also included in the alignment. The putative carboxyl group-binding residues are *highlighted* with *stars* underneath the PSD-95 PDZ2 sequence, and the residue at the αB1 position is indicated with a *black dot*. The amino acid residues of PDZ7 that form the GRASP-1-binding hydrophobic surface are *shaded* with *gray boxes* (see Fig. 5). In the nomenclature of the sequences, the labeling *r*, *m*, *h*, *p*, and *f* represent "rat", "mouse", "human", "mosquito", and "fruitfly", respectively.

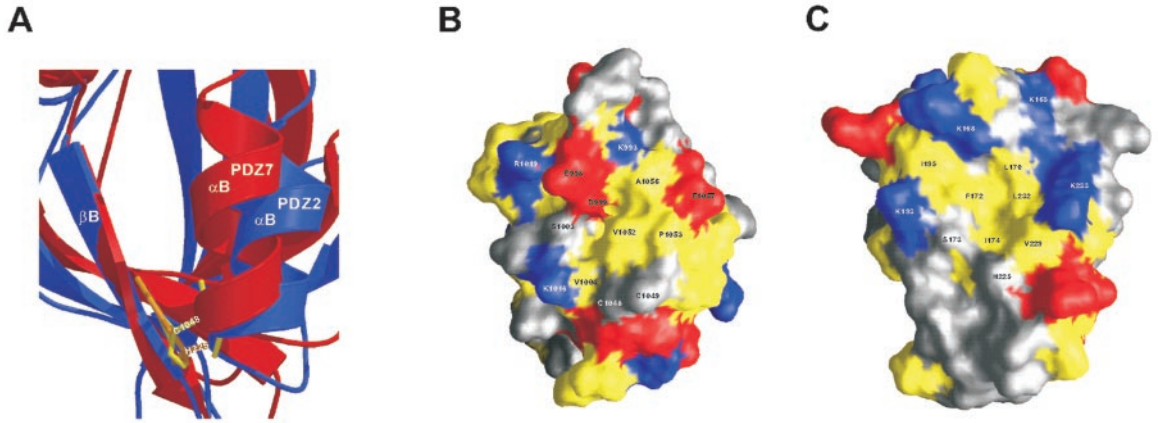

FIG. 3. **The GRIP1 PDZ7 contains a closed αB/βB-groove.** *A*, comparison of the αB/βB-groove conformation of GRIP1 PDZ7 to that of PSD-95 PDZ2. In this comparison, the two PDZ domains were superimposed with each other using their respective βB-strand. The amino acid residue in the αB1 position of each PDZ domain is drawn in explicit atom representations. *B* and *C*, surface representation of the αB/βB-grooves of GRIP1 PDZ7 (*B*) and PSD-95 PDZ2 (*C*). In this presentation, the hydrophobic amino acid residues are drawn in *yellow*, the positively charged residues in are shown in *blue*, the negatively charged residues are shown in *red*, and the uncharged polar residues are shown in *gray*. The orientations of the molecules in *B* and *C* are the same as shown in *A*. The surface diagram is generated using the program GRASP (37).

date a target carboxyl peptide, which is supposed to assume a β-strand conformation when binding to the PDZ domain. Additionally, the conformation of the carboxyl group-binding pocket of PDZ7 is not suited to interact with negatively charged carboxyl groups in the target peptides. The βA/βB-loop of PDZ7 (corresponding to the carboxyl group-binding

Downloaded from www.jbc.org at Hong Kong University of Science & Technology, on April 9, 2011

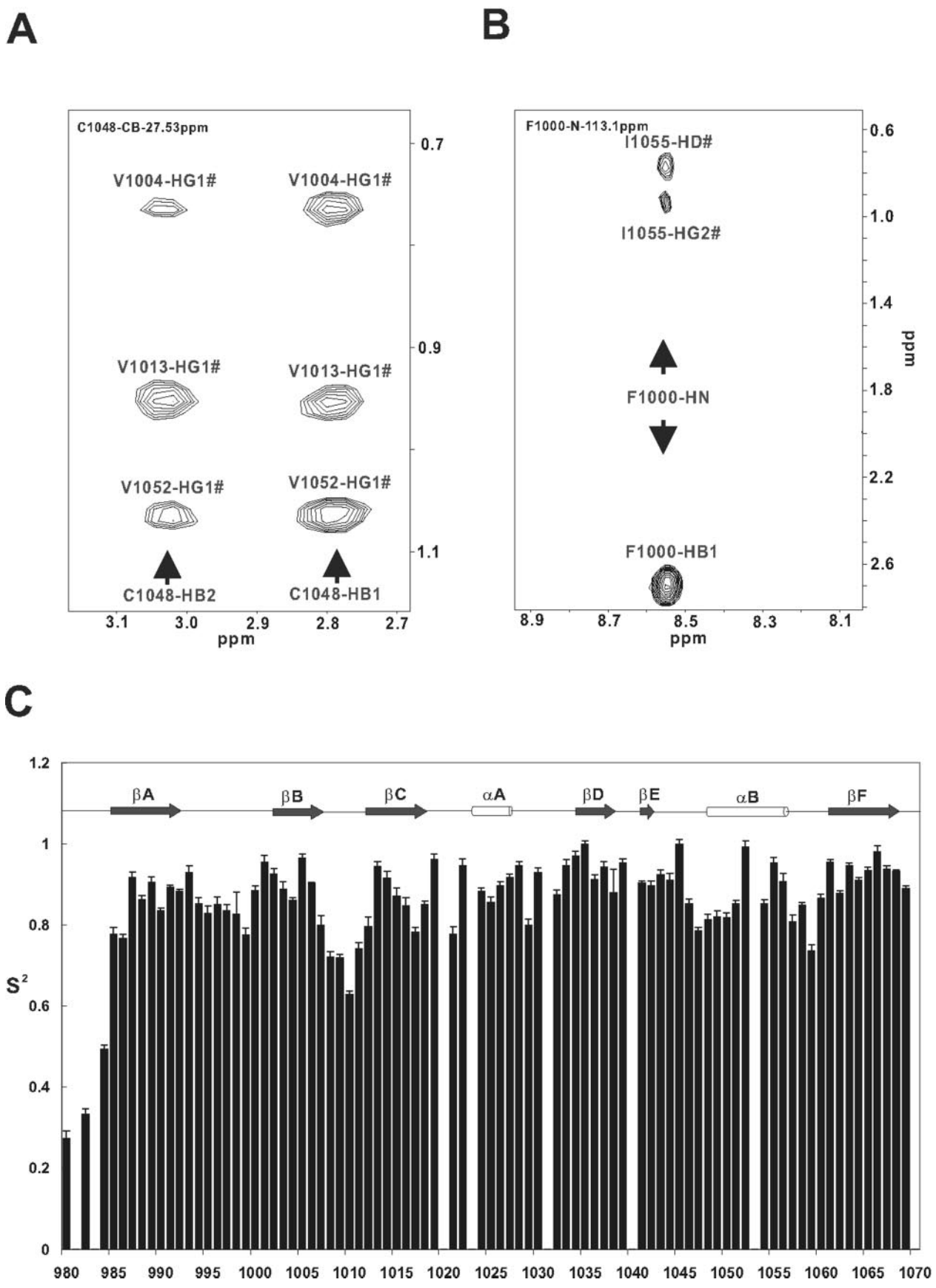

FIG. 4. **Characterization of the αB/βB-groove.** *A*, representative NOE contacts between Cys-1048 in the αB1 with the residues from βB and αB. The data is taken from a three-dimensional ^{13}C-separated NOESY spectrum of the protein at the Cβ chemical shift of Cys-1048. *B*, an ^{15}N-NOESY strip showing NOE contacts between the backbone amide proton of Phe-1000 in the DFGF-loop with Ile-1055 at the end of αB of PDZ7. *C*, backbone amide-order parameters (S^2) of GRIP1 PDZ7 determined by NMR relaxation experiments. The S^2 values were derived from T_1, T_2, and ^{1}H-^{15}N NOE values of GRIP1 PDZ7 measured on field strength of 500 MHz. For easy comparison, the secondary structure of the protein is included in the figure.

Downloaded from www.jbc.org at Hong Kong University of Science & Technology, on April 9, 2011

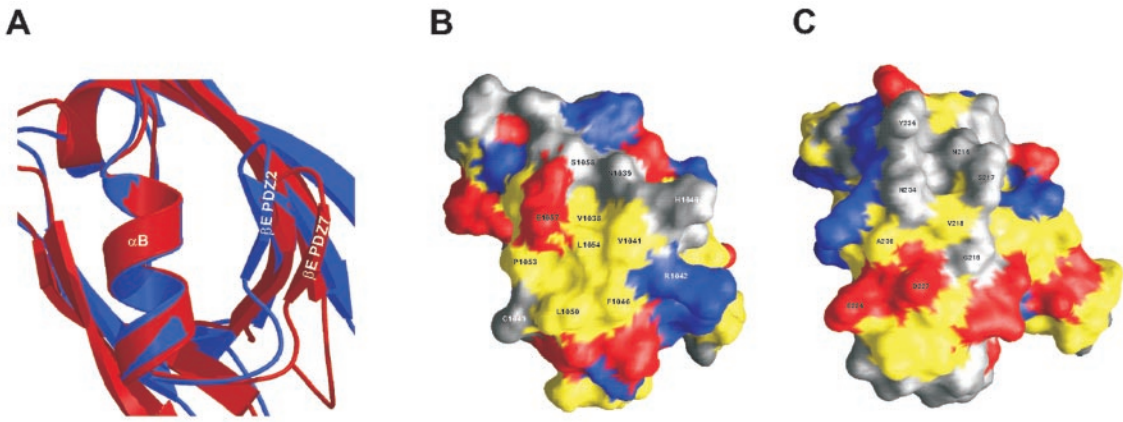

FIG. 5. **The βE/αB-hydrophobic surface of GRIP1 PDZ7.** *A*, comparison of the βE/αB-region conformation of GRIP1 PDZ7 to that of PSD-95 PDZ2. To simplify the comparison, the αB-helices of the two PDZ domains are superimposed with each other. *B* and *C*, surface representation of the βE/αB-grooves of GRIP1 PDZ7 (*B*) and PSD-95 PDZ2 (*C*) using the same coloring scheme in Fig. 3. The orientations of the molecules in *B* and *C* are the same as shown in *A*.

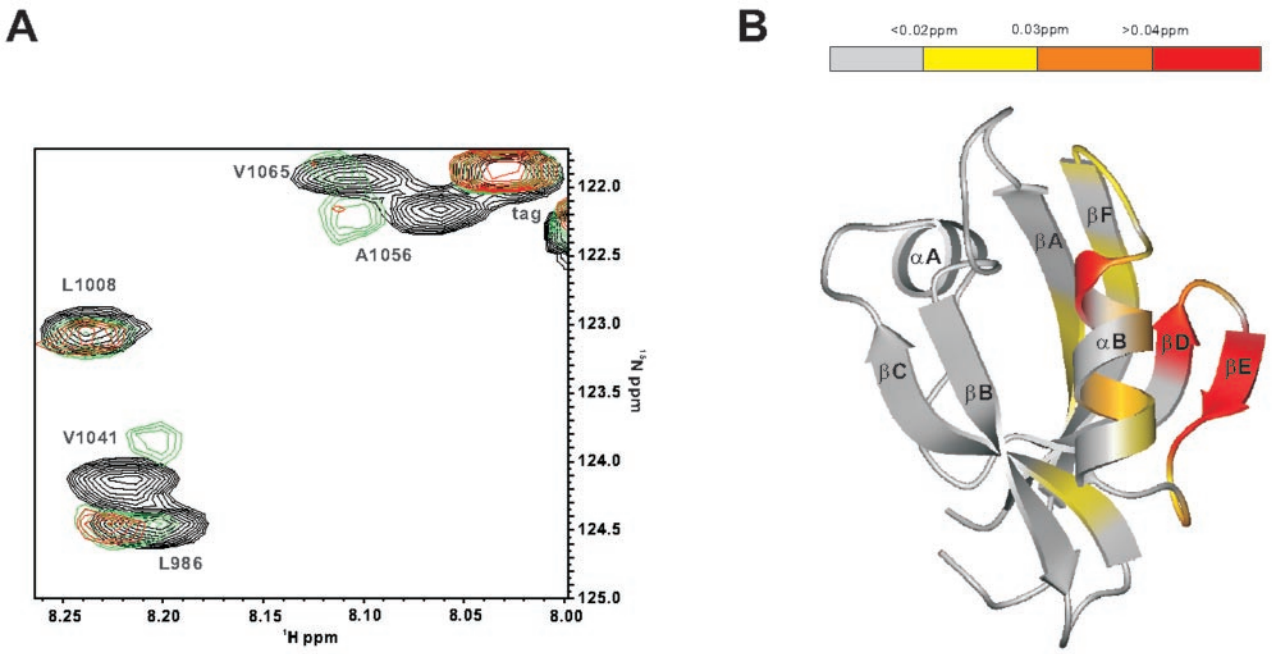

FIG. 6. **The βE/αB-hydrophobic surface-mediated interaction between GRIP1 PDZ7 and GRASP-1.** *A*, a selected region of the ^{1}H-^{15}N chemical shift correlation spectra of ^{15}N-labeled PDZ7 titrated with unlabeled GRASP-1, showing the interaction between the two proteins. In this diagram, the backbone amide peaks of the free PDZ7 are shown in *black*, and the amide peaks of PDZ7 in the presence of 1:1 and 1:2 molar ratios of GRASP-1 are drawn in *green* and *red*, respectively. *B*, summary of the chemical shift changes of GRIP1 PDZ7 resulting from GRASP-1 binding. The combined ^{1}H and ^{15}N chemical shift changes are defined as

$$\Delta_{ppm} = \sqrt{(\Delta\delta_{HN})^2 + (\Delta\delta_N \cdot \alpha_N)^2}$$

The scaling factor (α_N) used to normalize the ^{1}H and ^{15}N chemical shifts is 0.17. The coloring scheme is presented using a *horizontal bar* on the *top* of the figure. The figure is prepared using the program MOLMOL.

loop of conventional PDZ domains) contains two additional residues (Fig. 2). The conformation of this loop is largely defined (Fig. 1*A*) by a number of NOE contacts between amino acid residues from this loop with those from the COOH-terminal end of the αB helix (see Fig. 4*B* for an example). The limited conformational freedom of the βA/βB-loop is also supported by the order parameter values (S^2) of the backbone amides in this region measured from the NMR relaxation experiments (Fig. 4*C*). Fig. 3, *B* and *C*, compares the surface structures of the αB/βB-grooves of PDZ7 and PSD-95 PDZ2. Because of the packing of the βA/βB-loop with the αB helix, PDZ7 does not have a hydrophobic pocket to accommodate the side chain of the target peptide residue at the 0 position (Fig. 3*B*). Additionally, a highly conserved positively charged residue that functions to stabilize the negative charge of the carboxyl group of target peptide (Lys-233 in PSD-95 PDZ2) (Fig. 3*C*) is missing in PDZ7. Instead, several negatively charged residues (Glu-998, Asp-999, and Glu-1057) surround the remaining small hydrophobic surface in PDZ7 (Fig. 3*B*). Taken together, we conclude that the GRIP1 PDZ7 αB/βB-groove adopts a closed conformation. We predict that GRIP1 PDZ7 is not likely to be able to interact with carboxyl peptides using its αB/βB-groove. Consistent with our prediction, no proteins with classical PDZ-binding

Downloaded from www.jbc.org at Hong Kong University of Science & Technology, on April 9, 2011

carboxyl termini were found to interact with GRIP1 PDZ7 in a recent yeast two-hybrid screening (21).[2] However, we cannot rule out the possibility that GRIP1 PDZ7 may undergo a large conformational change in the αB/βB region, rendering an interaction of the domain with carboxyl peptides.

GRIP PDZ7 Contains a Distinct Hydrophobic Surface Formed by βE/αB—Structural analysis shows that the space between the backbones of αB and βE of PDZ7 is larger than that of PSD-95 PDZ2 (as well as other PDZ domains with known structures) (Fig. 5*A*). A prominent hydrophobic surface formed by amino acid residues from βE to αB can be observed in PDZ7 (Fig. 5*B*). We term this hydrophobic surface as the βE/αB-surface. The entire αB helix of GRIP PDZ7 is composed of hydrophobic amino acid residues, and it contributes four residues (Cys-1049, Leu-1050, Pro-1053, and Leu-1054) to the βE/αB-hydrophobic surface (Figs. 2 and 5*B*). Furthermore, the amino acid residues forming the βE/αB-hydrophobic surface are highly conserved in both GRIP1 and GRIP2 (Fig. 2). Such hydrophobic surface is not observed in other PDZ domains including PSD-95 PDZ2 (Fig. 5*C*). It is possible that GRIP1 PDZ7 may use the βE/αB-hydrophobic surface rather than the αB/βB-groove to interact with its binding partner(s).

GRASP-1 Binds to PDZ7 via the βE/αB-hydrophobic Surface—The binding of GRASP-1 to GRIP1 PDZ requires a ~100-residue fragment at the COOH-terminal end of GRASP-1, and this 100-residue PDZ7-binding domain of GRASP-1 contains neither a classical PDZ-binding motif at its carboxyl terminus nor a PDZ-like fold (21). Preliminary NMR and circular dichroism spectroscopic studies of the purified COOH-terminal 100-residue PDZ7-binding domain of GRASP-1 indicated an α-helix-rich structure, and the domain forms a large molecular multimer in solution (data not shown). We titrated ^{15}N-labeled PDZ7 with the unlabeled PDZ7-binding domain of GRASP-1. The addition of substoichiometric amounts of GRASP-1 resulted in chemical shift as well as peak intensity changes of a number of backbone amides of PDZ7 (Fig. 6*A*), confirming that GRASP-1 indeed interacts with GRIP1 via direct binding to its PDZ7 domain (21). The data in Fig. 6*B* summarizes the backbone amide chemical shift changes of PDZ7 induced by GRASP-1 binding. The amino acid residues at the COOH-terminal end of βD, the whole βE as well as part of αB facing the βD/βE-strands, experience the largest amplitude of GRASP-1-induced chemical shift changes. The region that shows obvious GRASP-1-induced chemical shift changes closely overlaps with the βE/αB-hydrophobic surface shown in Fig. 5*B*, indicating that GRASP-1 binds to PDZ7 via the distinct βE/αB-hydrophobic surface. In contrast, we do not observe any GRASP-1-induced chemical shift changes of the residues in the "DFGF-loop" (the conventional carboxyl group-binding motif) as well as those in the entire βB-strand (Fig. 6). In addition, no chemical shift changes could be detected for the Cys-1048 in the αB1 position of PDZ7 upon the addition of GRASP-1. Taken together, the chemical shift perturbation data indicate that the conventional target-binding groove (*i.e.* the βB/αB-groove) is not involved in GRASP-1 binding. Chemical shift perturbation data also indicate that GRASP-1 binding induces localized conformational changes to PDZ7 (in the βE/αB-region). To our knowledge, the data presented here demonstrate for the first time that a PDZ domain can interact with its target via a site distinct from the well characterized target-binding βB/αB-groove.

PDZ domain-mediated dimerization/multimerization is a common feature for a number of PDZ domain proteins. It is possible that a PDZ domain may dimerize and/or multimerize via the βE/αB-hydrophobic surface seen in GRIP1 PDZ7 (30–33). Further work is ongoing to directly prove or refute whether some of the above mentioned PDZ domain multimerizations are indeed mediated via the βE/αB-hydrophobic surface seen in GRIP1 PDZ7. In addition, it will be interesting to experimentally test whether other atypical PDZ domain-mediated interactions such as CLP-36 PDZ binding to spectrin-like repeats of α-actinin (39) are mediated via the βE/αB-hydrophobic surface.

In summary, the three-dimensional structure of GRIP1 PDZ7 determined in this work shows that the PDZ domain has a deformed βB/αB-groove that is not likely to be capable of binding to carboxyl peptide ligands. Instead, GRIP1 PDZ7 contains a distinct hydrophobic surface largely composed of the residues from the βE to αB regions of the protein. Unexpectedly, GRIP1 PDZ7 binds to its target GRASP-1 via the βE/αB-hydrophobic surface instead of the conventional target-binding βB/αB-groove. The novel protein-binding surface revealed in this work may help us to understand the molecular basis of frequently observed PDZ domain-mediated multimerization of multimodular scaffold proteins.

Acknowledgments—We thank Drs. Richard Huganir and Morgan Sheng for providing cDNA constructs of GRASP-1 and GRIP1 and Dr. Virginia Unkefer for critical reading of the paper.

[2] R. Huganir, personal communication.

REFERENCES

1. Schultz, J., Copley, R. R., Doerks, T., Ponting, C. P., and Bork, P. (2000) *Nucleic Acids Res.* **28,** 231–234
2. Craven, S. E., and Bredt, D. S. (1998) *Cell* **93,** 495–498
3. Harris, B. Z., and Lim, W. A. (2001) *J. Cell Sci.* **114,** 3219–3231
4. Sheng, M., and Sala, C. (2001) *Annu. Rev. Neurosci.* **24,** 1–29
5. Morais Cabral, J. H., Petosa, C., Sutcliffe, M. J., Raza, S., Byron, O., Poy, F., Marfatia, S. M., Chishti, A. H., and Liddington, R. C. (1996) *Nature* **382,** 649–652
6. Doyle, D. A., Lee, A., Lewis, J., Kim, E., Sheng, M., and MacKinnon, R. (1996) *Cell* **85,** 1067–1076
7. Schultz, J., Hoffmuller, U., Krause, G., Ashurst, J., Macias, M. J., Schmieder, P., Schneider-Mergener, J., and Oschkinat, H. (1998) *Nat. Struct. Biol.* **5,** 19–24
8. Daniels, D. L., Cohen, A. R., Anderson, J. M., and Brunger, A. T. (1998) *Nat. Struct. Biol.* **5,** 317–325
9. Tochio, H., Zhang, Q., Mandal, P., Li, M., and Zhang, M. (1999) *Nat. Struct. Biol.* **6,** 417–421
10. Songyang, Z., Fanning, A. S., Fu, C., Xu, J., Marfatia, S. M., Chishti, A. H., Crompton, A., Chan, A. C., Anderson, J. M., and Cantley, L. C. (1997) *Science* **275,** 73–77
11. Hillier, B. J., Christopherson, K. S., Prehoda, K. E., Bredt, D. S., and Lim, W. A. (1999) *Science* **284,** 812–815
12. Tochio, H., Mok, Y. K., Zhang, Q., Kan, H. M., Bredt, D. S., and Zhang, M. (2000) *J. Mol. Biol.* **303,** 359–370
13. Dong, H., O'Brien, R. J., Fung, E. T., Lanahan, A. A., Worley, P. F., and Huganir, R. L. (1997) *Nature* **386,** 279–284
14. Wyszynski, M., Valtschanoff, J. G., Naisbitt, S., Dunah, A. W., Kim, E., Standaert, D. G., Weinberg, R., and Sheng, M. (1999) *J. Neurosci.* **19,** 6528–6537
15. Srivastava, S., Osten, P., Vilim, F. S., Khatri, L., Inman, G., States, B., Daly, C., DeSouza, S., Abagyan, R., Valtschanoff, J. G., Weinberg, R. J., and Ziff, E. B. (1998) *Neuron* **21,** 581–591
16. Dong, H., Zhang, P., Song, I., Petralia, R. S., Liao, D., and Huganir, R. L. (1999) *J. Neurosci.* **19,** 6930–6941
17. Bruckner, K., Pablo Labrador, J., Scheiffele, P., Herb, A., Seeburg, P. H., and Klein, R. (1999) *Neuron* **22,** 511–524
18. Lin, D., Gish, G. D., Songyang, Z., and Pawson, T. (1999) *J. Biol. Chem.* **274,** 3726–3733
19. Torres, R., Firestein, B. L., Dong, H., Staudinger, J., Olson, E. N., Huganir, R. L., Bredt, D. S., Gale, N. W., and Yancopoulos, G. D. (1998) *Neuron* **21,** 1453–1463
20. Bladt, F., Tafuri, A., Gelkop, S., Langille, L., and Pawson, T. (2002) *Proc. Natl. Acad. Sci. U. S. A.* **99,** 6816–6821
21. Ye, B., Liao, D., Zhang, X., Zhang, P., Dong, H., and Huganir, R. L. (2000) *Neuron* **26,** 603–617
22. Delaglio, F., Grzesiek, S., Vuister, G. W., Zhu, G., Pfeifer, J., and Bax, A. (1995) *J. Biomol. NMR* **6,** 277–293
23. Garrett, D. S., Powers, R., Gronenborn, A. M., and Clore, G. M. (1991) *J. Magn. Reson.* **95,** 214–220
24. Bax, A., and Grzesiek, S. (1993) *Acc. Chem. Res.* **26,** 131–138
25. Kay, L. E., and Gardner, K. H. (1997) *Curr. Opin. Struct. Biol.* **7,** 722–731
26. Wüthrich, K. (1986) *NMR of Proteins and Nucleic Acids*, John Wiley & Sons, Inc., New York
27. Farrow, N. A., Muhandiram, R., Singer, A. U., Pascal, S. M., Kay, C. M., Gish, G., Shoelson, S. E., Pawson, T., Forman-Kay, J. D., and Kay, L. E. (1994) *Biochemistry* **33,** 5984–6003
28. Cornilescu, G., Delaglio, F., and Bax, A. (1999) *J. Biomol. NMR* **13,** 289–302
29. Brunger, A. T., Adams, P. D., Clore, G. M., DeLano, W. L., Gros, P., Grosse-

Downloaded from www.jbc.org at Hong Kong University of Science & Technology, on April 9, 2011

Kunstleve, R. W., Jiang, J. S., Kuszewski, J., Nilges, M., Pannu, N. S., Read, R. J., Rice, L. M., Simonson, T., and Warren, G. L. (1998) *Acta Crystallogr. Sec. D* **54,** 905–921
30. Zhang, Q., Fan, J. S., and Zhang, M. (2001) *J. Biol. Chem.* **276,** 43216–43220
31. Xu, X. Z., Choudhury, A., Li, X., and Montell, C. (1998) *J. Cell Biol.* **142,** 545–555
32. Fouassier, L., Duan, C., Feranchak, A. P., Yun, C. H., Sutherland, E., Simon, F., Fitz, J. G., and Doctor, R. B. (2001) *Hepatology* **33,** 166–176
33. Lau, A. G., and Hall, R. A. (2001) *Biochemistry* **40,** 8572–8580
34. Koradi, R., Billeter, M., and Wuthrich, K. (1996) *J. Mol. Graph.* **14,** 51–55
35. Kraulis, P. J. (1991) *J. Appl. Crystallogr.* **24,** 946–950
36. Merritt, E., and Murphy, M. (1994) *Acta Crystallogr. Sec. D* **50,** 869–873
37. Nicholls, A. (1992) *GRASP: Graphical Representation and Analysis of Surface Properties*, Columbia University, New York
38. Laskowski, R. A., Rullmannn, J. A., MacArthur, M. W., Kaptein, R., and Thornton, J. M. (1996) *J. Biomol. NMR* **8,** 477–486
39. Vallenius, T., Luukko, K., and Makela, T. P. (2000) *J. Biol. Chem.* **275,** 11100–11105

Downloaded from www.jbc.org at Hong Kong University of Science & Technology, on April 9, 2011